



## The Evolution of Parasite Virulence and Transmission Rate in a Spatially Structured Population

YOSHIHIRO HARAGUCHI AND AKIRA SASAKI\*

*Department of Biology, Faculty of Science, Kyushu University, Fukuoka 812-81, Japan*

*(Received on 27 April 1999, Accepted in revised form on 14 December 1999)*

If the transmission occurs through local contact of the individuals in a spatially structured population, the evolutionarily stable (ESS) traits of parasite might be quite different from what the classical theory with complete mixing predicts. In this paper, we theoretically study the ESS virulence and transmission rate of a parasite in a lattice-structured host population, in which the host can send progeny only to its neighboring vacant site, and the transmission occurs only in between the infected and the susceptible in the nearest-neighbor sites. Infected host is assumed to be infertile. The analysis based on the pair approximation and the Monte Carlo simulation reveal that the ESS transmission rate and virulence in a lattice-structured population are greatly reduced from those in completely mixing population. Unlike completely mixing populations, the spread of parasite can drive the host to extinction, because the local density of the susceptible next to the infected can remain high even when the global density of host becomes very low. This demographic viscosity and group selection between self-organized spatial clusters of host individuals then leads to an intermediate ESS transmission rate even if there is no tradeoff between transmission rate and virulence. The ESS transmission rate is below the region of parasite-driven extinction by a finite amount for moderately large reproductive rate of host; whereas, the evolution of transmission rate leads to the fade out of parasite for small reproductive rate, and the extinction of host for very large reproductive rate.

© 2000 Academic Press

### Introduction

The classical theory of the evolution of parasites argues that the virulence and transmission rates evolve to maximize the basic reproductive ratio of the parasite (for example, May and Anderson, 1983). This hypothesis is by no means always applicable to all circumstances. For example, superinfection of parasites (Axelrod & Hamilton, 1981; Bremermann & Pickerling, 1983; Frank, 1992; Levin & Pimentel, 1981; May & Nowak, 1995; Sasaki, 1994; Sasaki & Iwasa, 1991) leads to

a higher ESS virulence because the intra-host competition among strains favors a more virulent parasite than that which maximizes the basic reproductive ratio. The virulence evolved in expanding population should be larger than that in population in demographic plateau (Lenski & May, 1995). Spatial structure is also a factor likely to affect the ESS transmission rate and virulence of parasite. However, there has been little attempt to take the spatial structure explicitly into account when examining the evolution of the parasite (Claessen & de Roos, 1995; Rand *et al.*, 1995). Spatially explicit models have also been used to analyse the evolution of cooperation (Matsuda *et al.*, 1992; Nakamaru

\* Author to whom correspondence should be addressed.  
E-mail: [asasascb@mbox.nc.kyushu-u.ac.jp](mailto:asasascb@mbox.nc.kyushu-u.ac.jp)

*et al.*, 1997; Nowak & May, 1992) are allelopathy (Durrett & Levin, 1997; Iwasa *et al.*, 1998).

Epidemiological dynamics in spatially structured populations has been shown to be different from the classical ones without spatial structure. Sato *et al.* (1994) studied the epidemiological dynamics in a lattice-structured population using pair approximation, which keeps track of the spatial correlation between the nearest-neighbor sites. The most important finding for the equilibrium states of the population was that the parasite could drive the host to extinction. The conditional probabilities or local densities (e.g. the probability that a susceptible host is the nearest neighbor of an empty site) play a critical part in determining the invasibility and the persistence of infected in the population. If the transmission rate is sufficiently large, the host goes to extinction, a result which is never found in a completely mixing population. The parasite can spread in the disease-free host population without reducing greatly the local density of susceptibles at the nearest neighbor to an infected. Sato *et al.* (1994) have shown that local density of susceptibles around each infected remains high enough to allow the local expansion of the infected individual even if the global density of host approaches zero. As a result, the susceptible population goes to extinction before the local density of infected individuals around them falls. In a completely mixing population, in contrast, decreased host density will immediately result in a reduced mean transmission rate, which stops the population from going extinct. This large difference in demographic outcomes between spatial and non-spatial models leads us to expect that the optimal life history of a parasite will be different when we explicitly take into account the spatial structure. Here we will examine the evolution of the parasite in a lattice-structured population.

In a closely related model, Rand *et al.* (1995) have examined how spatial structure affects the evolution of transmission rate. Their observations of Monte Carlo simulations suggested that the transmission rate of parasite evolves toward the upper limit for the persistence of the parasite. This is in contrast to the ESS transmission rate without host spatial structure, in which the transmission rate increases without limit if there is no

tradeoff between the transmission rate and the additional mortality caused by infection. We will discuss later the differences in the assumptions and results between our model and that of Rand *et al.* (1995).

Our study is also motivated by the finding that the degree of local and global transmissions is related to the severity of disease caused by infectious bacteria in humans (Ewald, 1991). We therefore focus on how the ESS virulence depends on the mobility of the host and the parasite, and will examine what demographic factor is the primarily important one in modeling the course and the outcome of virulence evolution.

The model assumed in this paper is the same as in Sato *et al.* (1994) except that we introduce an additional mortality due to infection (virulence) and allow mutation on the transmission rate of parasite. The present paper, however, highlights the evolution of parasite in spatially structured population, as well as the demographic consequence of spatially explicit model in epidemiology. The population consists of a regular lattice, with each site being either empty, occupied by susceptible, or occupied by an infected. A site becomes empty if an individual dies, and an empty site may be reoccupied by the progeny of one of the susceptibles in the nearest-neighbor sites. Transmission also occurs locally—a susceptible host may become infected from contact by an infected host in its nearest-neighbor site. We also assume a tradeoff between the transmission rate and the additional mortality of infected (virulence). Throughout the paper, we focus on the relationship between population demography and evolution. In the following analysis based on the pair approximation (Keeling *et al.*, 1997; Matsuda *et al.*, 1992; Sato *et al.*, 1994) and the Monte Carlo simulation, we will obtain the ESS transmission rate/virulence in a lattice structured, or viscous, population and will compare the result to those of a completely mixing population. We discuss how the reduced ESS virulence in viscous population can be understood from the spatial demography and spatial correlation structure. We also examine the evolution of virulence in simulated serial passage experiments, to examine in detail the effect of the self-clustering structure of infected individuals on the ESS virulence.

### Model

Let us consider the host population in a lattice-structured population, where each site of the lattice is either empty, occupied by a susceptible, or occupied by an infected. An  $L \times L$  regular lattice with a periodic boundary is assumed so that each site has four nearest neighbors. The state of the  $x$ -th site in the lattice at time  $t$  is denoted by  $\sigma_x(t) \in \{0, S, I\}$ , where the states 0,  $S$ , and  $I$  indicate, respectively, that the site is empty, occupied by a susceptible, and occupied by an infected host. When we consider the evolution of parasites, we introduce the state  $I_j$  which indicates that the site is occupied by an individual infected by the  $j$ -th strain of parasite.

A continuous time Markov process is defined by specifying the transition probability of each site in a unit time interval. The state of the  $x$ -th site changes by

(i) the mortality of a susceptible:

$$S \rightarrow 0, \quad \text{at rate } d_1 (= 1), \quad (1)$$

(ii) the mortality of an infected:

$$I \rightarrow 0, \quad \text{at rate } d_2 (= 1 + \alpha), \quad (2)$$

(iii) the reproduction of susceptibles:

$$0 \rightarrow S, \quad \text{at rate } rn_x(S)/z, \quad (3)$$

(iv) infection:

$$S \rightarrow I, \quad \text{at rate } \beta n_x(I)/z, \quad (4)$$

where  $n_x(\sigma)$  represents the number of sites with the state  $\sigma$  in the nearest neighbor of the  $x$ -th site, and  $z$  is the number of nearest-neighbor sites ( $z = 4$  for a regular lattice). The mortality of a susceptible and that of an infected are denoted by  $d_1$  and  $d_2$ , where time is scaled so that the mortality of a susceptible host  $d_1$  equals 1 (i.e. the mean lifetime of a susceptible is 1),  $\alpha = d_2 - d_1$  is the additional mortality (virulence) of an infected host,  $r$  is the reproduction rate of a susceptible of sending progeny to its nearest-neighbor sites,  $\beta$  is the transmission rate of parasite. We assume that the pathogen sterilizes a host immediately after infection.

### PHASE DIAGRAM OF EPIDEMIOLOGICAL PROCESS

The characteristics of the model is that both the host and the parasite tend to be clumped spatially because the host can only send progeny to its nearest-neighbor sites, and the parasite can only infect susceptibles next to an infected individual. Due to this self-organized clustering of the host and the parasite, the conventional epidemiological model that ignores spatial correlation fails to predict the demographic consequence and the evolutionary outcomes. We here summarize the possible equilibrium states of the population. Sato *et al.* (1994) have obtained, for the case of  $d_1 = d_2$ , a phase diagram in  $r$  and  $\beta$  parameter space based on the pair approximation, a technique which keeps track of the spatial correlation of the nearest-neighbor sites (Keeling *et al.*, 1997; Levin & Durrett, 1996; Matsuda *et al.*, 1992). Here we consider an additional parameter  $\alpha$ , the additional mortality due to infection, and followed the same analysis of the improved (i.e. partly incorporating triplet correlation) pair approximation by Sato *et al.* (1994) (see Appendix A for details). We also carried out extensive Monte Carlo simulations to examine the accuracy of the prediction made by pair approximation.

#### *The Phase Diagram*

As illustrated in Fig. 1, the pair approximation predicts that there are three kinds of equilibrium states. In the disease-free region, the parasite cannot invade the susceptible population because the transmission rate is smaller than the threshold for invasion. In the endemic region for intermediate transmission rates, the host and the parasite coexist. In the parasite-driven extinction region for sufficiently large transmission rates, the susceptible hosts go to extinction by the spread of the parasite, leading to the extinction of the whole population. Note that the parasite-driven extinction region never appears in non-spatial epidemic models. The intuitive reason why the parasite can cause the host extinction in viscous population is that the local density of susceptibles in the neighborhood of the infected remains high even when the global density approaches zero, which can be verified by the analysis of equilibrium pair densities (Sato *et al.*, 1994).

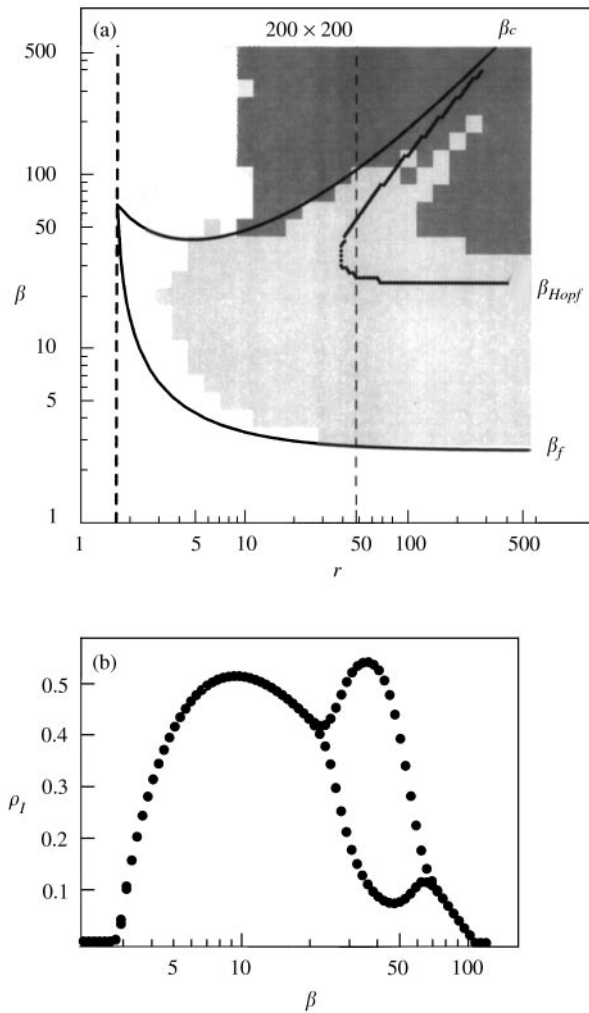


FIG. 1. Equilibrium states of epidemiological process in lattice-structured population, predicted from the pair approximation and observed in Monte Carlo simulations. (a) The curves represent two threshold transmission rates,  $\beta_c$  and  $\beta_f$ , as a function of host reproduction rate  $r$ , predicted from the pair approximation (see Appendix A). If  $\beta > \beta_c$  the parasite will drive the host to extinction; if  $\beta_f < \beta < \beta_c$  the population is endemic; and if  $\beta < \beta_f$  the parasite cannot invade the disease-free population. The gradation in the background indicates the most frequently observed equilibrium state in simulation of five independent replicates with  $100 \times 100$  regular lattice. The outcome of each simulation run is classified into endemic (light gray, both susceptibles and infected individuals persisted until  $t = 50$ ), disease-free (dark gray, infected individuals went to extinction, leaving disease-free population) and parasite-driven host extinction (white, susceptibles went to extinction, leading to the extinction of entire population). This curve shows the region within which the endemic equilibrium is locally unstable, leading to limit cycles in pair density dynamics. (b) The maximum and minimum densities of infected host, after initial transient period, obtained by numerical differentiation of pair density dynamics (Appendix A). As  $\beta$  increases past the first threshold the supercritical Hopf bifurcation occurs, and the subcritical Hopf bifurcation occurs at the second threshold. Parameters: (a)  $d_1 = 1.0$ ,  $\alpha = 1.0$ ; (b)  $d_1 = 1.0$ ,  $r = 48.0$ ,  $\alpha = 1.0$ .

The process of parasite-driven extinction (PDE) is a deterministic one—the host and parasite densities steadily decrease toward zero and one cannot prevent the population from going extinct by increasing the lattice size. This makes a sharp contrast to the epidemic fade-out, in which (parasite) extinction due to finite population size occurs when the infected density hits zero in a damping oscillation. PDE is also a characteristic of sterilizing parasites as assumed in the present model. However, it is a robust phenomenon in the sense that the PDE region remains even if infected hosts reproduce but with a lower rate than that of susceptible (Boots & Sasaki, 1999).

Monte Carlo simulations of  $100 \times 100$  lattice populations support the predictions from pair approximation (Fig. 1). However, there are some discrepancies between the predicted and simulated results. Firstly, the region for parasite-driven extinction observed in Monte Carlo simulations is wider than that predicted by pair approximation. Secondly, the simulations reveals an additional disease-free region for sufficiently small reproductive rate of the host and a sufficiently high transmission rate, a region for which the pair approximation predicts population extinction. Both deviations can be ascribed to the effect of density fluctuation in finite population (i.e. epidemic fade out). Indeed, the pair approximation predicts limit cycles where population extinction occurred in Monte Carlo simulations for high host reproductive rate in the endemic region (Fig. 1), and a large periodical component is observed in the trajectories for low host reproductive rate [Fig. 3(b), (c)].

### Evolution of Virulence in Viscous Population

In a completely mixing population, it has been shown (May & Anderson, 1983) that the parasite trait evolves to maximize the basic reproduction ratio:

$$R_0 = \frac{\beta}{d_1 + \alpha}.$$

This implies that if the additional mortality  $\alpha$  of the infected host and the transmission rate  $\beta$  are independent of each other,  $\beta$  evolves to infinity

and  $\alpha$  evolves to zero. However, if this criteria were to remain true for the spatially structured populations examined in this paper, the evolution of the parasite transmission rate would lead to the extinction of host population, as the epidemiological parameters enter in the region for parasite-driven extinction (see Fig. 1). Our objective in this section is to examine how the criteria for the ESS transmission rate and virulence change in lattice-structural populations, and what the consequence of the evolution of epidemiological parameters is to the demographic stability and persistence of the population.

Let us consider a parasite population consisting of two different strains with different transmission rates—the wild type with transmission rate  $\beta_I$  and the additional mortality  $\alpha_I$ , and a mutant with  $\beta_J$  and  $\alpha_J$ . By modifying the doublet density dynamics described in Appendix A to include two strains of the parasite (but ignoring double infection), we see that the global density of mutant parasite strain,  $\rho_J$  changes when rare as

$$\frac{d\rho_J}{dt} = (\beta_J q_{S/J} - d_1 - \alpha_J) \rho_J, \quad (5)$$

where  $q_{S/J} = p_{S/J}/\rho_J$  is the local density of susceptible ( $S$ ) in the nearest neighbor of a mutant infected host ( $J$ ). Let  $q_{S/J} = q_{S/I} + \Delta q_{S/J(I)}$  and noting that  $q_{S/I} = (d_1 + \alpha_I)/\beta_I$  at equilibrium of wild-type infected population, the marginal growth rate of the mutant can be written as

$$\lambda(J/I) = \beta_J \left\{ \frac{d_1 + \alpha_I}{\beta_I} - \frac{d_1 + \alpha_J}{\beta_J} + \Delta q_{S/J(I)} \right\}. \quad (6)$$

Thus, if the mutant parasites are surrounded by more susceptibles than the wild-type parasites (i.e. if  $\Delta q_{S/J(I)} > 0$ ), the mutant can invade even when it has a lower basic reproductive ratio (Table 1). Because lower transmission rate and lower virulence make the local density of susceptible around an infected increase, the expression suggests that viscous populations favor lower transmission rate and lower virulence through the  $\Delta q$  term. Note that the mechanism does not require any group selection argument, although one may be able to interpret the same results from the viewpoints of inter-cluster selection (i.e.

TABLE 1

	$\beta$	$\alpha$	$R_0$	$q_{S/J}, q_{S/I}$	$\lambda(J/I)$
(a)					
Mutant ( $J$ )	25	1	12.5	0.081	0.038
Resident ( $I$ )	30	1	15.0	0.066	—
(b)					
Mutant ( $J$ )	30	1	15.0	0.062	-0.14
Resident ( $I$ )	25	1	12.5	0.080	—

The basic reproductive ratio  $R_0$  and local susceptible density of an infected ( $q_{S/I}$  and  $q_{S/J}$ ), for resident and mutant strains differing in transmission rates  $\beta$ . Local densities  $q_{S/I}$  and  $q_{S/J}$  are the long-term averages observed in Monte Carlo simulation.  $q_{S/I}$  is calculated by counting the number of nearest-neighbor pairs with the states  $S-I$  and divided by the number of  $I$ -sites, which is averaged over the time interval before the mutant is introduced.  $q_{S/J}$  is obtained from the interval where the mutant is rare. (a) The mutant strain with a lower basic reproductive ratio invades and replaces the resident strain. The mutant has a higher local density of susceptibles than the resident,  $\Delta q = q_{S/J} - q_{S/I} > 0$ , giving a positive marginal growth rate  $\lambda(J/I) > 0$  calculated from eqn (6) in the text. (b) Quantities for the same pair of strains with the reversed roles. The mutant with a higher basic reproductive ratio cannot invade. The host reproduction rate  $r = 10.0$ , and the death rate of susceptible  $d_1 = 1$ .

the argument relying on the self-organized clusters of individuals as units of selection).

#### VISCOUS POPULATION FAVORS MILD PATHOGEN

We here explore the evolutionarily stable transmission rate  $\beta$  and virulence  $\alpha$  if many strains with different  $\beta$  and  $\alpha$  compete in a regular lattice population. As before, we assume that the reproduction of susceptibles occurs by sending progeny to the nearest-neighbor empty site, and that a susceptible host may become infected if there is an infected host as its nearest neighbor. If there are several different strains of parasites as nearest neighbors of a susceptible, the transmission of a particular strain occurs with a probability proportional to the number of hosts infected by that strain, weighted by the transmission rate of the strain. As for the trade-offs between transmission rate and additional mortality, we assume two of the simplest relationships: (i) the additional mortality is independent of the transmission rate; (ii) the additional mortality is proportional to the transmission rate:  $\alpha_i = c\beta_i$  for each strain  $i$  with a positive constant  $c$ . Note that the ESS transmission rate is infinity in a

completely mixing population with either of the above relationships.

#### *ESS Transmission Rate Without Trade-off*

Figures 2 and 3 show typical evolutionary trajectories for the population mean transmission rate in the case of constant additional mortality ( $\alpha_i = 1$ ). As the natural mortality of host  $d_1$  is scaled to 1, this means that the mortality of infected hosts is twice as large as that of susceptibles. For a fixed host reproduction rate, the mean transmission rate increases from a low value in the initial population, and reaches a plateau.

When overlaid on the phase diagram in  $r$ - $\beta$  parameter space [Fig. 4(a)], the transmission rate stops increasing before the parameters enter the region of parasite-driven extinction from the endemic region. Extensive simulations for different reproductive rates of susceptibles reveal that the ESS transmission rate for moderately large reproductive rate is below the parasite-driven-extinction region by a finite amount (i.e. the ESS transmission rate is not arbitrary close to the threshold for host extinction, and hence the endemic equilibrium is stably maintained in the evolutionary stable population). We should note, however, that for sufficiently high host reproductive rate, the evolution of transmission rate may result in population extinction due to the finiteness of population size and large fluctuation of population densities. In contrast, for sufficiently small host reproductive rate, the evolution could lead to the extinction of parasite, leaving only susceptible hosts.

In a lattice-structured population, the host has a clumped distribution due to its local reproduction. If there is no trade-off between transmission and mortality, a parasite with a very high transmission rate enjoys an advantage in spreading within a cluster. However, there would be a correspondingly low transmission probability between clusters, because it will tend to infect all the susceptibles in the cluster, leading to local extinction before transmitting to other clusters of susceptibles. Thus, an intermediate transmission rate should evolve in a viscous population even if the transmission rate is independent of the other epidemiological parameters.

#### *Virulence Increasing Linearly with Transmission Rate*

Similar results are obtained if we assume a linear trade-off between virulence and transmission rate. In this case the prediction from the complete mixing population is the evolution of an infinite transmission rate and virulence, but this never occurs in simulations in a lattice population. Figure 4(b) shows the phase diagram in the parameter space of additional mortality  $\alpha$  and transmission rate  $\beta$  for a fixed reproduction rate. The spatial structure leads to the evolution of an intermediate transmission rate and virulence.

#### SERIAL PASSAGE EXPERIMENTS

It is well known that parasites tend to increase their virulence as an outcome of serial passage through cell culture (Doroshenko *et al.*, 1996; John & John, 1994). Our theory predicts that the destruction of clustering structure in space in such procedures should increase the ESS transmission rate and virulence in a serially passaged population. To confirm this we conducted simulations for the evolution of transmission rate and virulence in a population that mimics the serial passage experiments.

In simulations, the infected host population may include a number of different strains. We do not consider any trade-off between transmission rate and mortality of infected host. Starting from the introduction of a small number of parasites to a host population inhabiting a regular lattice, we change clusters if the proportion of infected host reached 10% of the total lattice. In changing clusters, we randomly sampled 10% of the infected hosts (that may include various parasite strains), and introduced them into a new medium which consists only of the susceptible host and empty sites. In each simulation, we cultivated 500–600 passages.

Comparison of the mean transmission rates in serial passage and in normal lattice population shows a striking difference (Fig. 5)—in the serial passage the mean transmission rate continued to increase and exceeded 150, for the same parameters in which the ESS transmission rate in normal lattice population balances around 20. When introduced to a new medium in the serial passage experiments, the parasite finds a high

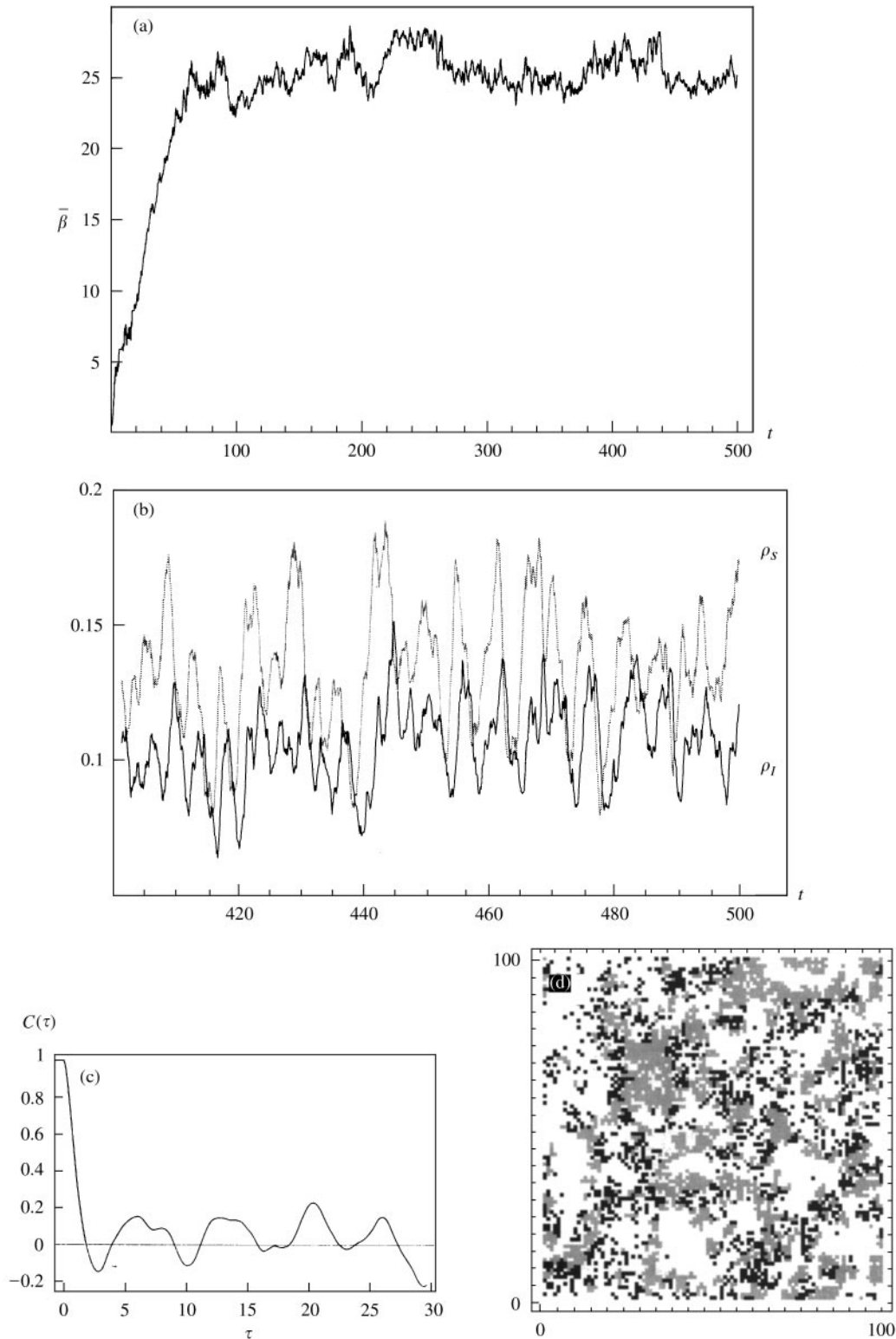


FIG. 2. The simulation results for the evolution of transmission rate of parasite. We assume that the parasite population may consist of 30 different strains with equally divided transmission rate  $\beta$  from  $\beta_{min} = 0.4$  to  $\beta_{max} = 80.0$ . Each strain may change by mutation to a strain of adjacent mutation rate at a rate of 0.1. The top panel shows the change in the population mean transmission rate, and the middle panel shows the trajectories of global densities of susceptibles (gray line) and infected individuals (black line) from  $t = 400$  to 500. The bottom left panel shows the autocorrelation of the density of infected individuals against lag  $\tau$  averaged over the last half-time interval. The bottom right panel shows a snapshot from the simulation of the spatial configuration of sites, where gray and black cell, respectively, represent the site occupied by susceptible and infected host, and blank cell represents vacant site. The size of lattice is  $100 \times 100$ . (a):  $d_1 = 1.0, r = 8.0, \alpha = 1.0$ .

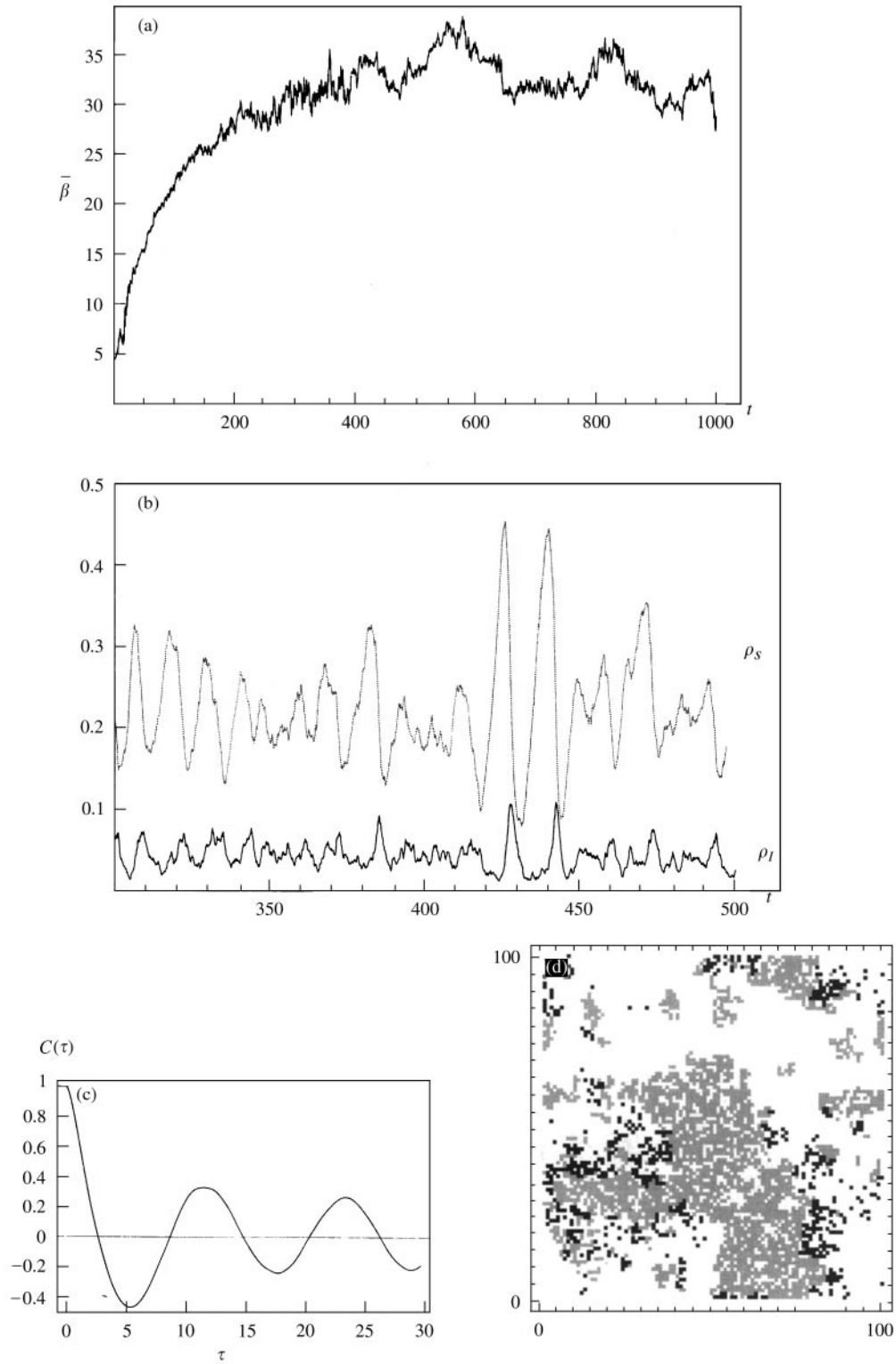


FIG. 3. The same as Fig. 2, with parameters  $d_1 = 1.0$ ,  $r = 4.0$ ,  $\alpha = 1.0$ .

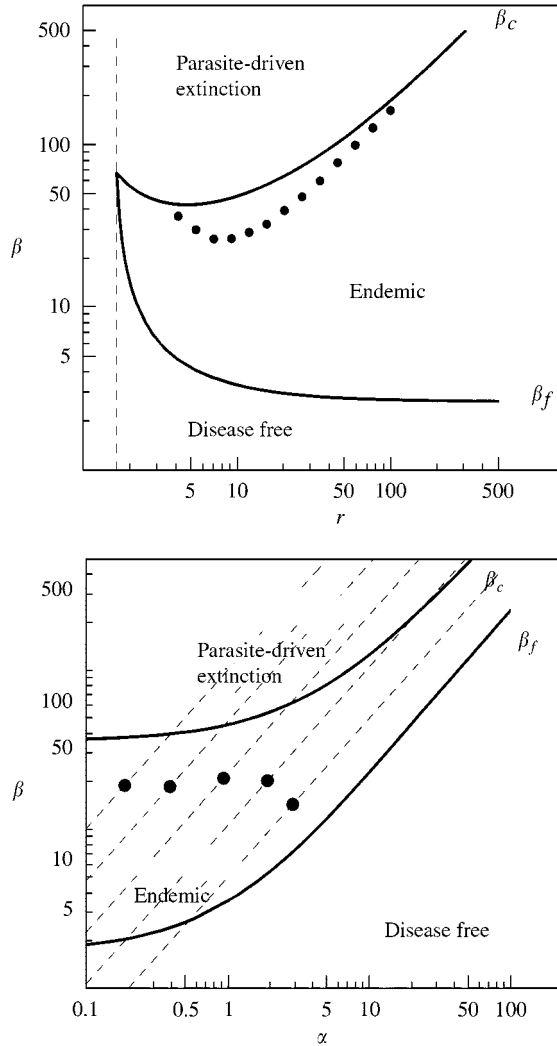


FIG. 4. The evolutionarily stable transmission rate of parasite for a given host reproduction rate. (a) The results of Monte Carlo simulations for the evolution of transmission rate in  $200 \times 200$  lattice. We allow 101 strains of parasite with equally divided transmission rate from  $\beta_{min} = 5.0$  to  $\beta_{max} = 200.0$ . The simulation starts with the introduction of the parasite strain with the minimum transmission rate, and allowed to evolve for 500 host generations (i.e. until  $t = 500$ , as the mean lifetime of a susceptible host is  $1/d_1 = 1$ ), where a parasite strain can mutate to one of the adjacent strains at a rate of 0.5 per host generation. For each value of host reproductive rate (horizontal axis), the long-term average of the population mean transmission rate over last 50 generations are plotted (dots). Curves represent two threshold transmission rates predicted from pair approximation. When the host reproductive rate is smaller than 4, the evolutionary increase of transmission rate led to the extinction of parasite; whereas, when it is larger than 100, the evolution led to the extinction of host population. Otherwise, the parasite transmission rate stopped increasing fairly below the threshold for population extinction (note logarithmic scale). (b) The evolutionarily stable transmission rate  $\beta$  and virulence  $\alpha$ , when there is a linear trade-off:  $\alpha = c\beta$ . The coefficient  $c$  of trade-off varied from 0.01 to 0.2, and the

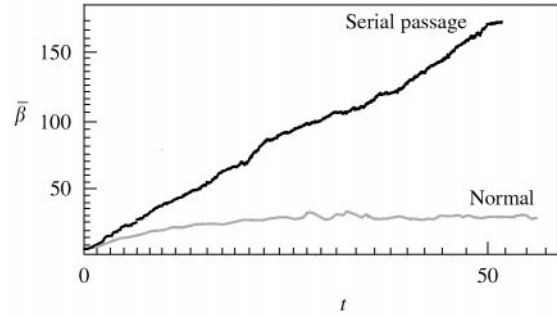


FIG. 5. The evolutionary trajectory of the mean transmission rate of parasite in serial passage model (bold) and normal lattice model (gray). In both models, the parasite transmission rate is allowed to change by mutation (see legends of Figs 2 and 4). In the simulation of serial passage model, whenever the density of infected host exceeded 10% of total population, 10% of infected individuals are randomly chosen and are introduced into a new lattice population consisting only of susceptible and vacant sites. The mean transmission rate of parasite continues to increase in serial passage model, while it balances at a low value in normal lattice model with the same parameters. The size of lattice is  $100 \times 100$ .  $d_1 = 1.0$ ,  $r = 8.0$ ,  $\alpha = 1.0$ .

density of susceptibles because the population was disease free. Hence, even if the pathogen has a very high transmission rate, the local density of susceptible around the infected is sufficiently large, and the strain with higher transmission rate can invade, as is predicted from eqn (6) with  $\Delta q$  negligibly small.

## Discussion

We have shown that the ESS transmission rate and virulence in a lattice-structured population is significantly smaller than that in a completely mixing population. Most strikingly, the ESS transmission rate is finite even if there is no trade-off between transmission and virulence. The reason why a higher transmission rate without any cost is not always favored in spatially structured population can be ascribed to two

← pairs of transmission rate and virulence constrained by trade-off are shown by broken lines. For a given trade-off, transmission rate and virulence evolve along the broken lines, and balance at intermediate values (dots) within the region of endemic equilibrium. The size of lattice is  $200 \times 200$ . Parameters: (a)  $d_1 = 1.0$ ,  $\alpha = 1.0$ ; (b)  $d_1 = 1.0$ ,  $r = 8.0$ .

factors. First, the “self-shading” of infected hosts reduces the effective transmission rate in viscous population—as the transmission occurs only between individuals in the nearest neighbour sites, a local increase of infected individuals immediately results in a decrease of susceptibles in the vicinity. The self-shading is more significant for a parasite with higher transmission, because the infected individuals quickly fill a cluster of susceptibles. The second factor is that the susceptible hosts form a self-organized clustering structure, dividing the environment for parasites into small pieces of patches. Parasites having high transmission spread too fast in local patches, causing local extinction of a cluster before transmitting to another cluster of susceptibles.

Our result is related to the findings of “structured” (spatial or non-spatial) host–parasite models. Lipsitch *et al.* (1995) found that repeated contacts to the same partnership of hosts reduces the effective transmission rate, decreasing the ESS virulence for a given trade-off. Claessen & de Roos (1995) considered the evolution of virulence in a lattice-structured population. Their model neglects vacant sites and the site open by mortality is immediately filled by a susceptible. Because vacant site (or host density) plays a very important role in the demography and evolution of parasite, it is not surprising that their model shows no difference from the mean field on the ESS virulence in the single infection case. Rand *et al.* (1995) has analysed a model similar to ours and found that there is a critical transmissibility above which pathogen goes to extinction (leaving disease-free host population), and that the transmission rate evolves towards the criticality. They assumed that all host mortality is due to parasite virulence and hence susceptibles never die, but otherwise the model is the same as ours. Nevertheless, a striking difference exists in the results—they have not observed the parasite-driven extinction of host population. We found that the parameters which Rand *et al.* (1995) examined in their Monte Carlo simulations fall in the region of low host reproductive rate in our phase diagram (Fig. 1). Our analysis based on pair-approximation and Monte Carlo simulations reveal that increasing transmission rate for moderate or high host reproductive rates will lead to the extinction of the host population, rather than a

disease-free equilibrium. Their assertion on the evolution towards criticality should be clarified. Based on our analysis the ESS transmission rate is strictly below the threshold for population extinction, and for sufficiently large lattice size the population remains endemic at evolutionary stable state. In a small population, however, the evolution of transmission rate could lead to the extinction of both host and parasite, or parasite alone, depending on the host reproduction rate.

Well-known trends of the increase of virulence in serial passage experiments (Doroshenko *et al.*, 1996; John & John, 1994) can be ascribed to the destruction of spatial structure in serial passage procedure, which favors high virulence according to our model. In the same vein, we conjecture that pathogens that infect mobile cells (e.g. monocytes) would be more virulent than those which infect the sessile tissue culture.

There is a positive correlation between the virulence (disease-induced mortality) and the fraction of waterborne transmissions for infectious bacteria parasite in human population (Ewald, 1991, 1993). Highly virulent bacteria had a high fraction of waterborne transmissions. For example, *Vibrio cholerae* classical biotype and *Shigella dysenteriae* type I causing, respectively, 15.7 and 7.5% mortality in infected hosts, had high fractions of waterborne outbreaks (more than 80%). On the other hand, avirulent pathogen (Enterotoxigenic *Escherichia coli*, *Campylobacter jejuni* and non-typhoid salmonella, which cause less than 0.1% mortality) had low fractions of waterborne outbreaks (2–20%), mainly transmitted by contagion. Assuming that epidemics with waterborne transmissions would be approximated by completely mixing model, and that with contagious transmission by local transmission model, our theory predicts that much higher virulence would evolve for pathogens with waterborne transmission. The present paper only deals with two extreme modes of transmissions. A more general model should address the ESS virulence as functions of the fraction of short-range and long-range transmission or the spectrum of transmission distance (Boots & Sasaki, 1999).

We thank Kenji Ikeda for discussion, and Mike Boots for useful comments.

## REFERENCES

- AXELROD, R. & HAMILTON, W. D. (1981). The evolution of cooperation. *Science* **211**, 1390–1396.
- BOOTS, M. & SASAKI, A. (2000). “Small worlds” and the evolution of virulence: infection occurs locally and at a distance. *Proc. R. Soc. London B* **266**, 1933–1938.
- BREMERMAN, H. J. & PICKERLING, J. (1983). A game-theoretical model of parasite virulence. *J. theor. Biol.* **100**, 411–426.
- CLAESSEN, D. & DE ROOS, A. (1995). Evolution of virulence in a host-pathogen system with local pathogen transmission. *Oikos* **74**, 401–413.
- DOROSHENKO, E. P., VASIL'eva & KISELEVA, A. K. (1996). The virulence of *Yersinia pestis* strains in serial-passage in guinea pig peritoneal macrophages. *Zhurnal Mikrobiologii, Epidemiologii i Immunobiologii* **1**, 14–16.
- DURRETT, R. & LEVIN, S. A. (1997). Allelopathy in spatially distributed populations. *J. theor. Biol.* **185**, 165–171.
- EWALD, P. W. (1991). Waterborne transmission and the evolution of virulence among gastrointestinal bacteria. *Epidemiol. Infect.* **106**, 83–119.
- EWALD, P. W. (1993). The evolution of virulence. *Sci. Am.* **264**, 56–62.
- FRANK, S. A. (1992). A kin selection model for the evolution of virulence. *Proc. R. Soc. London B* **250**, 195–197.
- IWASA, Y., NAKAMARU, M. & LEVIN, S. A. (1998). Allelopathy of bacteria in a lattice population: competition between colicin-sensitive and colicin-producing strains. *Evol. Ecol.* **12**, 785–802.
- JOHN, D. T. & JOHN, R. A. (1994). Enhancement of virulence of *Naegleria fowleri* by growth in Vero-cell culture. *J. Parasitol.* **80**, 149–151.
- KEELING, M. J., RAND, D. A. & MORRIS, A. J. (1997). Correlation models for childhood epidemics. *Proc. R. Soc. London B* **264**, 1149–1156.
- LENSKI, R. & MAY, R. M. (1995). The evolution of virulence: a reconciliation between two conflicting hypotheses. *J. theor. Biol.* **169**, 253–265.
- LEVIN, S. & DURRETT, R. (1996). From individuals to epidemics. *Proc. R. Soc. London B* **351**, 1615–1621.
- LEVIN, S. & PIMENTEL, D. (1981). Selection of intermediate rates of increase in parasite–host systems. *Am. Nat.* **117**, 308–315.
- LIPSITCH, M., HERRE, E. A. & NOWAK, M. A. (1995). Host population structure and the evolution of virulence: a “law of diminishing returns”. *Evolution* **49**, 743–748.
- MATSUDA, H., OGITA, N., SASAKI, A. & SATO, K. (1992). Statistical mechanics of population—the lattice Lotka–Volterra model. *Prog. Theor. Phys.* **88**, 1035–1049.
- MAY, R. M. & ANDERSON, R. M. (1983). Epidemiology and genetics in the coevolution of parasites and hosts. *Proc. R. Soc. London B* **219**, 281–313.
- MAY, R. R. & NOWAK, M. A. (1995). Coinfection and the evolution of parasite virulence. *Proc. R. Soc. London B* **261**, 209–215.
- NAKAMARU, M., MATSUDA, H. & IWASA, Y. (1997). The evolution of cooperation in a lattice-structured population. *J. theor. Biol.* **184**, 65–81.
- NOWAK, M. A. & MAY, R. M. (1992). Evolutionary games and spatial chaos. *Nature* **359**, 250–253.
- RAND, D. A., KEELING, M. & WILSON, H. B. (1995). Invasion, stability and evolution to criticality in spatially extended, artificial host–pathogen ecology. *Proc. R. Soc. London B* **259**, 55–63.
- SASAKI, A. (1994). Evolution of antigen drift/switching: continuously evading pathogens. *J. theor. Biol.* **168**, 291–308.
- SASAKI, A. & IWASA, Y. (1991). Optimal growth schedule of pathogens within a host: switching between lytic and latent cycles. *Theor. Popul. Biol.* **39**, 201–239.
- SATO, K., MATSUDA, H. & SASAKI, A. (1994). Pathogen invasion and host extinction in lattice structured populations. *J. Math. Biol.* **32**, 251–268.

## APPENDIX A

## Pair Approximation

In this appendix we derive the pair approximation of the model. The analysis is analogous to that of Sato *et al.* (1994) except that we added a new parameter  $\alpha$ , the additional mortality of infected. There are three states in each site: empty (0), susceptible (S), and infected (I). Let  $\rho_\sigma(t)$  be the probability that a randomly chosen site has the state  $\sigma$  at time  $t$ , and  $p_{\sigma\sigma'}$  be the probability that a randomly chosen pair of nearest-neighbor sites has state  $\sigma\sigma'$ . We can define the conditional density  $q_{\sigma|\sigma'}$  as the probability that a nearest neighbor of  $\sigma'$ -site has the state  $\sigma$ . Likewise,  $q_{\sigma'|\sigma''}$  represents the conditional probability that a nearest neighbor of  $\sigma'$  site in the  $\sigma'\sigma''$ -pair has the state  $\sigma$ . By definition we should have  $\sum_\sigma \rho_\sigma = 1$ ,  $\sum_\sigma \rho_{\sigma|\sigma'} = 1$  and

$$p_{\sigma\sigma} = \rho_\sigma q_{\sigma|\sigma}, \quad (\text{A.1})$$

$$p_{\sigma\sigma'} = \rho_\sigma q_{\sigma'|\sigma} = \rho_{\sigma'} q_{\sigma|\sigma'}, \quad \text{if } \sigma \neq \sigma'. \quad (\text{A.2})$$

We scale time so that the mortality of a susceptible is 1. From the transitions probabilities (1)–(4) in the text, the following differential equations for pair densities are derived:

$$\dot{p}_{00} = -2r(1-\theta)q_{S|00}p_{00} + 2(1+\alpha)p_{I0}, \quad (\text{A.3})$$

$$\begin{aligned} \dot{p}_{S0} = & -[1+r\{\theta+(1-\theta)q_{S|0S}\} \\ & +\beta(1-\theta)q_{I|S0}]p_{S0} + r(1-\theta)q_{S|00}p_{00} \\ & + p_{SS} + (1+\alpha)p_{IS}, \end{aligned} \quad (\text{A.4})$$

$$\begin{aligned} \dot{p}_{SS} = & -\{2+2(1-\theta)\beta q_{I|SS}\}p_{SS} \\ & + 2r\{\theta+(1-\theta)q_{S|0S}\}p_{S0}, \end{aligned} \quad (\text{A.5})$$

$$\begin{aligned}
\dot{p}_{I0} &= - [1 + \alpha + r\{\theta + (1 - \theta)q_{S/0I}\}]p_{I0} && \text{and} \\
&+ \beta(1 - \theta)q_{I/S0}p_{S0} + p_{IS} && q_{S/0I} = q_{S/0}, \\
&+ (1 + \alpha)p_{II}, && (A.6) \quad q_{S/00} = \varepsilon q_{S/0},
\end{aligned}$$

$$\begin{aligned}
\dot{p}_{IS} &= - [2 + \alpha + \beta\{\theta + (1 - \theta)q_{I/SI}\}]p_{IS} \\
&+ r(1 - \theta)q_{S/0I}p_{I0} + \beta(1 - \theta)q_{I/SS}p_{SS}, && (A.7)
\end{aligned}$$

$$\begin{aligned}
\dot{p}_{II} &= - 2(1 + \alpha)p_{II} \\
&+ 2\beta\{\theta + (1 - \theta)q_{I/SI}\}p_{IS}, && (A.8)
\end{aligned}$$

where dots represent the time derivative, and  $\theta = 1/z$ . As pair density dynamics depends on triplet densities (e.g.  $q_{I/SS}$ ), the following approximation for triplet correlation is used to complete the pair approximation:  $q_{I/S\sigma} = q_{I/S}$  for any  $\sigma$ ,

where  $\varepsilon$  is determined to be consistent with the threshold reproductive rate for the persistence of host in disease-free population, and is 0.8093 for two-dimensional regular lattice (Sato *et al.*, 1994). Phase diagram in Figs 1(a) and 4 are derived by examining the local stability of disease-free equilibrium and population extinction equilibrium as in Sato *et al.* (1994), using (A.4)–(A.8) (from the normalization relationship we can discard one of the equations from (A.3) to (A.8)). In addition, we examined the local stability of the endemic (internal) equilibrium of (A.4)–(A.8), and reveals the Hopf bifurcation points in parameter space [Fig. 1(b)].